Indonesian Journal of Material Research
e-ISSN: 2987-1654
Vol. 4, No. 3, November 2026

Indonesian Journal of MATERIAL RESEARCH

Research Paper

Influence of Carrier Localization, Recombination, and Dispersion on Carrier Dynamics in InGaN/GaN Quantum Wells

Nguyen Thi Phuong Loan[1*], Hsiao-Yi Lee[2], Phan Thi Minh Man[3]

[1] *Faculty of Fundamental 2, Posts and Telecommunications Institute of Technology, Ho Chi Minh City, 700000, Vietnam*
[2] *Department of Electrical Engineering, National Kaohsiung University of Sciences and Technology, Kaohsiung, 807618, Taiwan*
[3] *Faculty of Electrical and Electronics Engineering, Ton Duc Thang University, Ho Chi Minh City, 700000, Vietnam*
[*] **Corresponding author**: ntploan@ptithcm.edu.vn

Abstract
This study investigates carrier recombination dynamics in InGaN/GaN quantum wells using time-resolved techniques, including induced grating methods, time-resolved photoluminescence, and pump–probe spectroscopy. Diffusion and carrier lifespan dependency on excitation density is systematically analyzed for structures with varying indium compositions and barrier configurations. The results reveal that carrier lifetime decreases while diffusion coefficients increase with rising excitation density, indicating enhanced nonradiative recombination under high carrier concentrations. This behavior is more pronounced in samples with higher indium content, suggesting a strong influence of carrier localization. The experimental observations are interpreted using an extended ABC recombination model that incorporates carrier density–dependent recombination processes. The analysis demonstrates that defect-assisted recombination becomes dominant at high excitation levels, while Auger recombination remains negligible within the investigated carrier density range. Furthermore, pump–probe measurements confirm distinct recombination pathways associated with localized and delocalized carrier states. These findings provide important insights into the physical mechanisms governing carrier dynamics and performance droop in InGaN-based quantum well designs, offering guidance for the optimization of high-performance optoelectronic devices.

Keywords
Carrier Dynamics, InGaN/GaN Quantum Wells, Carrier Recombination, Carrier Localization, Time-Resolved Spectroscopy

Received: 15 March 2026, Accepted: 30 May 2026
https://doi.org/10.26554/ijmr.20264396

1. INTRODUCTION

InGaN/GaN quantum well (QW) structures have attracted extensive attention in recent decades due to their remarkable applications in high-efficiency light-emitting diodes (LEDs), laser diodes, and other optoelectronic devices. Their direct bandgap, high thermal stability, and tunable emission wavelength make them highly suitable for visible-light technologies. Despite the rapid development of InGaN-based LEDs, one of the most critical challenges limiting device performance is the so-called efficiency droop phenomenon, in which the internal quantum efficiency (IQE) decreases significantly under high injection current or high excitation density conditions (Kumar et al., 2018; Tain et al., 2015; Li and Li, 2011). This issue severely restricts the operation of high-power LEDs and has therefore become a major research topic in semiconductor physics and optoelectronic engineering.

Several methods have been proposed for explaining performance droop in InGaN/GaN quantum wells, including carrier leakage, electron overflow, junction heating, Auger recombination, and defect-assisted nonradiative recombination (Miyazaki and Kamei, 1988). Among these mechanisms, Auger recombination has long been considered one of the most probable origins of efficiency degradation because theoretical calculations predict relatively large Auger coefficients in InGaN materials under certain resonant conditions. However, many experimental studies have reported inconsistencies between theoretical predictions and measured carrier dynamics, suggesting that additional physical mechanisms may contribute significantly to efficiency droop. In particular, carrier localization caused by indium composition fluctuations and potential inhomogeneity in InGaN quantum wells has emerged as a key factor influencing recombination behavior, carrier transport, and diffusion processes (Shalamanov et al., 2019; Asano et al., 2012; Takamura and Kobayashi, 2002).

Previous investigations have primarily focused on electrically driven LED devices containing complex multi-quantum-well structures. Although these studies provide valuable information regarding practical device operation, electrical injection often introduces additional effects such as carrier overflow, contact resistance, and Joule heating, making it difficult to isolate the intrinsic carrier recombination mechanisms inside the quantum

wells. Consequently, there remains a need for systematic optical investigations capable of directly probing carrier dynamics without the influence of electrical injection. Furthermore, the interplay between carrier localization, carrier diffusion, and recombination pathways under varying excitation densities is still not fully understood, especially for structures with different indium compositions and barrier configurations.

To address these issues, this work investigates carrier recombination dynamics in InGaN/GaN quantum wells using several complementary time-resolved optical techniques, including induced grating measurements, time-resolved photoluminescence, and pump–probe spectroscopy. These techniques enable direct observation of carrier lifetime, diffusion behavior, and transient recombination processes under controlled excitation conditions. By systematically analyzing the dependence of carrier dynamics on excitation density, indium composition, and quantum well structure, this study aims to clarify the role of carrier localization and defect-assisted recombination in efficiency degradation. Based on previous reports, carrier localization and inner electric fields are believed to strongly influence carrier recombination rate and diffusion behavior in InGaN quantum wells (Dong et al., 2021; Chen et al., 2021; Shang et al., 2015).

The novelty of this work lies in the combined use of multiple time-resolved optical methods together with an extended ABC recombination analysis to distinguish the contributions of localized and delocalized carrier states in InGaN quantum wells. The results provide deeper insight into the physical mechanisms governing carrier transport and recombination, while also identifying the dominant nonradiative processes responsible for efficiency droop. These findings contribute to a more comprehensive understanding of carrier dynamics in InGaN-based materials and offer valuable guidance for the design and optimization of next-generation high-performance optoelectronic devices.

2. EXPERIMENTAL SECTION

2.1 Sample Preparation

This study examines two sets of samples. The first set consists of six structures fabricated on c-plane sapphire substrates using metal-organic vapor-phase epitaxy (MOVPE). A GaN buffer layer, barrier layers, and ten InGaN/GaN (L/G) quantum wells were sequentially grown. During the fabrication process, the TMIn/TMGa ratio was systematically varied to produce quantum wells with different indium compositions. Layer thicknesses were determined by X-ray diffraction, revealing variations in well thickness among the samples, whereas the barrier thickness remained constant. A reference structure without indium incorporation was also prepared under identical growth conditions. Photoluminescence (PL) analysis indicated that the indium content in the quantum wells varied over a broad range.

The second group consisted of dual-LED structures containing six-period quantum wells with fixed well thicknesses but variable barrier thicknesses, corresponding to both coupled and uncoupled multi-quantum-well (MQW) configurations. The LED architectures were fabricated using n-type GaN templates on sapphire substrates integrated with underlying Si-doped InGaN layers to improve carrier transport within highly excited active regions. In addition, step-graded electron injector structures composed of dual InGaN layers with progressively increasing indium content were introduced to enhance thermalization of hot carriers prior to injection into the active region. A p-type GaN cladding layer was subsequently deposited to complete the device structure (Reddy et al., 2017; Liang et al., 2011).

2.2 Instrumentation and Measurement Techniques

Unlike conventional pump-probe configurations that excite samples using Gaussian-like spatial profiles, the IGML technique employs an interference region generated by two coherent beams. This approach enables monitoring of transient grating dynamics through diffraction of a probe beam incident on the induced grating. One major advantage of this method is its ability to simultaneously evaluate carrier lifetime and diffusion behavior. In addition, because the IGML signal originates from diffraction efficiency, it is directly related to the spatial distribution of carrier density throughout the excitation depth, making the technique highly effective for probing instantaneous carrier-density dynamics. The IGML measurements utilized a frequency-tripled Nd:YAG laser emitting pulses at 355 nm with a duration of approximately 10 ns. The excitation power density was adjusted to control the carrier concentration during experiments. In the excitation scheme, a third-harmonic beam was employed to generate a transient grating on the sample using a holographic beam splitter (HBS). Due to the high absorption coefficient, only a shallow excitation depth was produced, resulting in elevated carrier densities (Zhao et al., 2020; Liu et al., 2015; Shin et al., 2013).

For time-resolved differential transmission measurements, a Ti:sapphire femtosecond laser source was employed. The output beam was divided into two equivalent components (Zou et al., 2018). One beam served as the pump pulse for optical excitation under continuously tunable wavelengths. The excitation was confined exclusively to the quantum wells (QWs), thereby avoiding carrier generation within the barrier, buffer, and cladding layers. The second beam acted as the probe pulse and was directed through a CaF_2 window to generate white-light illumination. This differential transmission technique enabled monitoring of carrier relaxation and redistribution processes in InGaN quantum wells with high temporal and spectral resolution.

For transient photoluminescence (TPS) analysis, a standard time-resolved PL setup was implemented using dual periodic pulses generated from a Ti:sapphire laser to selectively excite the QWs. Detection was carried out using a spectrometer coupled with a streak camera (Lu et al., 2019; Wang et al., 2015; Acuna et al., 2015). The system provided temporal resolution on the picosecond scale, and the delay between pump and probe pulses was systematically varied to investigate carrier relaxation dynamics. All measurements were conducted at room temperature unless otherwise stated.

2.3 Research Procedures

The carrier recombination dynamics were systematically investigated under different excitation densities to evaluate the dependence of carrier lifetime and diffusion behavior on carrier concentration. The excitation power density was gradually varied to monitor transient carrier relaxation processes in the InGaN/GaN quantum wells. Carrier lifetime and diffusion coefficients were extracted from induced grating measurements using transient diffraction signal analysis. Time-resolved photoluminescence and pump–probe spectroscopy were further employed to distinguish recombination pathways associated with localized and delocalized carrier states. All measurements were repeated under identical experimental conditions to ensure reproducibility and consistency of the obtained results.

3. RESULTS AND DISCUSSION

To investigate carrier transport and nonradiative recombination processes, the IGML signal was measured under varying excitation power. The excitation range was restricted by the signal-to-noise ratio at low power and by the onset of stimulated recombination at high power. Stimulated recombination acts as a fast recombination channel that rapidly depletes carriers once a critical excitation threshold is reached. Moreover, the IGML signal was analyzed under different transient grating conditions to extract both carrier lifetime and diffusion coefficients. Notably, the measured effective lifetime represents the combined contribution of multiple recombination processes, rather than the intrinsic carrier lifetime. The IGML decay observed in the reference GaN layer followed a nearly single-exponential behavior. In contrast, the experimentally measured IGML dynamics in InGaN were strongly influenced by excitation-related processes rather than solely by the intrinsic carrier lifetime. Nevertheless, under the weakest excitation condition, the decay behavior in the InGaN metallic component remained close to exponential, whereas slower decay components became dominant at longer time scales, reflecting the effective carrier lifetime.

The IGML dynamics in all InGaN layers gradually deviated from single-exponential behavior as the excitation intensity increased, while the initial decay component became faster at higher carrier densities. This effect was particularly pronounced in quantum wells containing larger indium concentrations and is commonly associated with complex recombination mechanisms that cannot be adequately described by simple recombination models. Such behavior is generally attributed to carrier-density-dependent recombination processes and is commonly interpreted using the ABC recombination model Li et al. (2018); Sun et al. (2017); Alaruri et al. (1993):

$$\frac{\partial N(x,z,t)}{\partial t} = D\nabla^2 N(x,z,t) - \frac{N(x,z,t)}{\tau_R} - BN^2(x,z,t) - CN^3(x,z,t) + G(x,z,t) \quad (1)$$

$G(x,z,t)$ signifies the carrier inducement pace. D signifies the ambipole dispersion coefficient. τ_R signifies the linearity. B and C signify the bi-granular and Auger recombination coefficients. It is possible to utilize expression (1) for assessing the refractivity indicator attunement $\Delta n(z,t) = n_{eh}\Delta N(z,t)$ (n_{eh} signifying the indicator variation caused via a carrier) as well as diffraction proficiency $\eta(t)$, empirically assessed via the IGML method:

$$\eta(t) = \left| \frac{2\pi}{\lambda_1} \int_0^d \Delta n(z,t)\, dz \right|^2 \quad (2)$$

The ABC model describes the recombination mechanisms through three components: Shockley-Read-Hall (A), radiative (B), and Auger (C) recombination. At low excitation densities, recombination is dominated by defect-related processes represented by the A coefficient. As the excitation density increases, radiative recombination becomes more significant, while Auger recombination remains negligible in the investigated regime. The observed decrease in carrier lifetime with increasing excitation density can therefore be attributed to enhanced nonradiative recombination associated with defect states and carrier localization effects.

The increase in diffusion coefficient at high excitation density suggests partial delocalization of carriers due to screening of localization potentials. Under low excitation conditions, carriers remain trapped within localized potential minima caused by indium fluctuations, resulting in longer carrier lifetime and reduced diffusion. As excitation density increases, these localized states become progressively filled, enabling carriers to occupy extended states with higher mobility. Consequently, carrier diffusion becomes more pronounced while nonradiative recombination channels are simultaneously enhanced.

The experimental observations are well described by the ABC model, where the increase in excitation density enhances defect-assisted recombination and reduces carrier lifetime. The absence of a strong Auger contribution indicates that efficiency droop in the investigated structures is primarily governed by defect-related recombination enhanced by carrier localization.

These results are consistent with previous studies, which reported that carrier localization significantly enhances nonradiative recombination and contributes to efficiency droop in InGaN-based quantum well structures. The simultaneous increase in diffusion coefficient and decrease in carrier lifetime indicates that carriers become more mobile at high excitation densities while recombination pathways are significantly enhanced.

The present findings are in good agreement with previous reports on InGaN/GaN quantum wells, where carrier localization was identified as a dominant factor influencing carrier transport and recombination dynamics (Li et al., 2018; Sun et al., 2017). Compared with earlier studies, the current work further demonstrates the strong excitation dependence of diffusion behavior and highlights the transition between localized and delocalized carrier states under increasing carrier density. This behavior supports the interpretation that defect-assisted nonradiative re-

combination becomes increasingly important at high excitation levels.

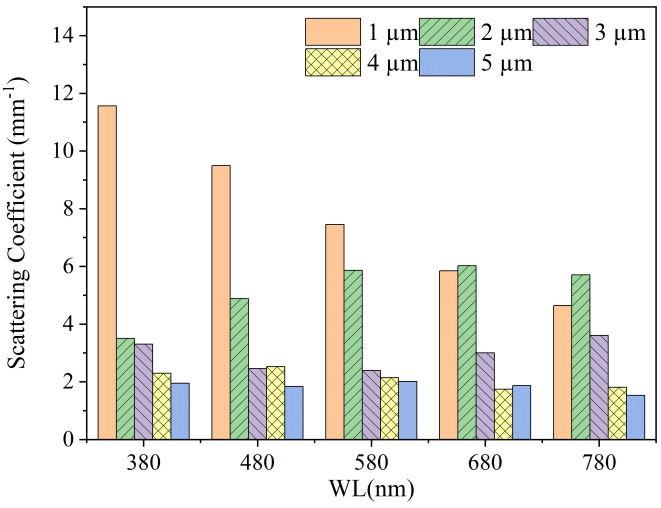

Figure 1. Relationship Between Scattering Coefficient and Wavelengths

The relationship between particle size and light distribution is seen in Figure 1. By increasing the effectiveness of wavelength conversion and light transmission, it can increase particle size. While forward emission blue light dispersion rises, blue illumination brightness may raise when forward scattering and reabsorption reduce. This is achieved by increasing particle size while reducing the amount of yellow phosphorus. In a similar vein, it is difficult to determine the ideal color temperature (CCT). Figures 2 and 3 demonstrate that CCT is independent of concentration.

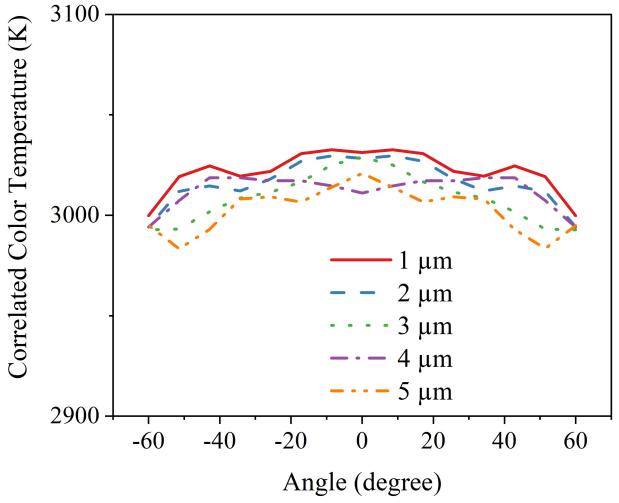

Figure 2. CCT Alteration Based on Various Particle Sizes

Increased doping can lower a phosphor's CCT variance, as seen in Figure 2. At temperatures of about 3025 K and particle sizes of 1 μm, the greatest CCT values are observed. The D-CCT reaches its lowest value of 40 K at a particle size of 5 μm, which is approximately 100 K lower than the value at 3 μm, which is about 140 K, as shown in Figure 3.

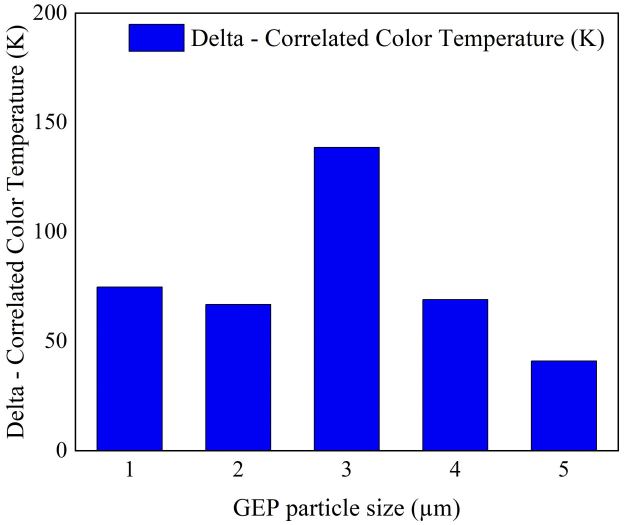

Figure 3. Variation in Hue Aberration Under Various Particle Sizes

Particle size does not always raise the brightness of white light emission, as shown in Figure 4. The best results of ~ 73 lm were obtained with particle sizes of 2 μm, whereas the worst results of ~ 71.5 lm were obtained with particle sizes of 4 μm. Reduced blue emission and an uneven color distribution result from increased backscattering and reabsorption. For instance, when exposed to more backscattered blue light, larger particle sizes may lead to the phosphor to change from blue to yellow or orange-red. For the phosphor coating to expand, a specific particle size is needed. The many reflections that the altered light would receive from different objects would limit the emitting spectrum. In other words, an elevated phosphor dose can raise the percentage of converted illumination that is back-reflected, increasing CCT while lowering luminous intensity. With a lumen output power of about 73 lm, Figure 4 shows how employing 2 μm particle sizes improved brightness and color uniformity in a simulated WLED (Juntunen et al., 2013).

Particle size significantly affects the brightness and hue rendering of white LEDs, as shown in Figures 5 and 6. As particle sizes grew from 1 to 5 μm, color rendition investigations employing the color rendering indicator (CRI) and the color quality scale (CQS) showed significant range in values. Lower CRI and CQS may be associated with the unpredictability of blue, green, and yellow-orange hues. High particle sizes lead to better dispersion and erratic light emission with a bias toward the yellow-orange spectrum. The CRI values fluctuates at around 56 while the CQS values rise from 39 to 41 with particle sizes of 1–2 μm, and then fluctuates at around 41 with particle sizes of 2–5 μm. We will modify this phosphor's CRI and CQS as we examine the data, taking into account additional elements like particle size.

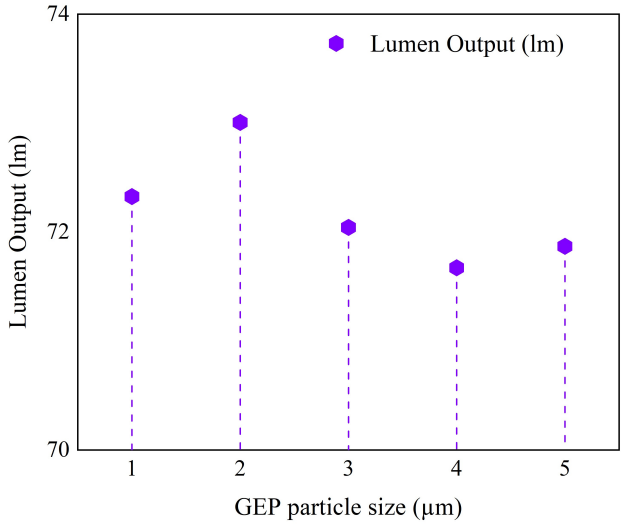

Figure 4. LED Lumen Generated Based on Various Particle Sizes

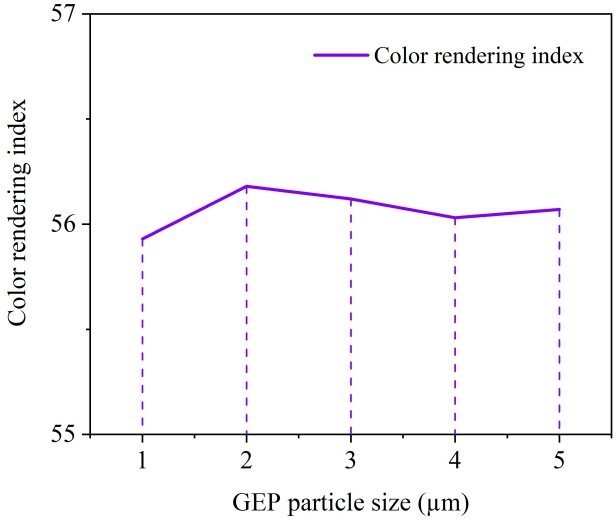

Figure 5. CRI Values with Various Particle Sizes

Despite the important insights obtained in this work, several limitations should be acknowledged. First, the measurements were mainly conducted at room temperature, whereas temperature-dependent investigations could provide additional information regarding thermal activation and carrier localization effects. Second, the excitation density range investigated in this study may not fully capture extremely high-density regimes where Auger recombination becomes more significant. In addition, direct structural characterization of defect distributions was beyond the scope of the present work. Future studies combining optical spectroscopy with advanced structural analysis techniques may provide a more comprehensive understanding of recombination mechanisms in InGaN/GaN quantum wells.

The findings of this study provide valuable guidance for improving the performance of InGaN-based optoelectronic devices. Understanding the relationship between carrier localization, diffusion behavior, and nonradiative recombination is essential for mitigating efficiency droop under high-power operating conditions. The results suggest that optimizing indium composition uniformity, defect density, and quantum well design could significantly improve carrier confinement and internal quantum efficiency in next-generation LED structures.

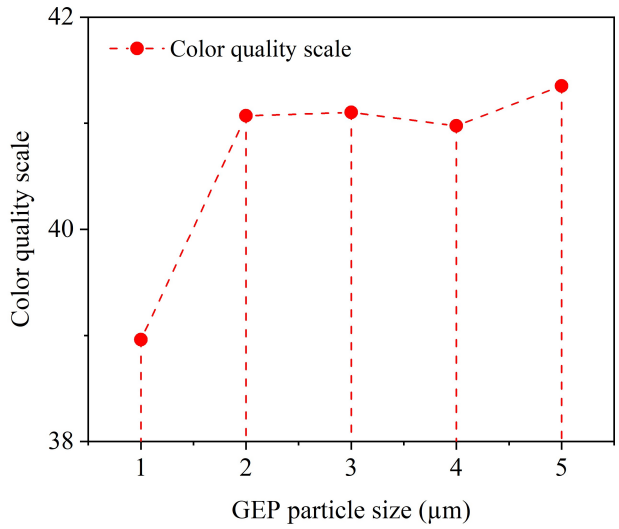

Figure 6. CQS Values with Various Particle Sizes

4. CONCLUSIONS

In this work, carrier recombination dynamics in InGaN/GaN quantum wells were systematically investigated using time-resolved optical techniques. The results demonstrate a strong dependence of carrier lifetime and diffusion behavior on excitation density, with increased nonradiative recombination observed at higher carrier concentrations. The findings highlight the critical role of carrier localization, particularly in structures with higher indium content, in governing recombination processes. By applying an extended ABC model, this study reveals that defect-assisted recombination is a dominant mechanism contributing to efficiency degradation, whereas Auger recombination plays a negligible role within the explored excitation regime. The combined analysis of induced grating and pump–probe measurements further distinguishes recombination dynamics between localized and extended carrier states. Overall, this work provides a clearer understanding of the interplay between carrier density, localization effects, and recombination pathways in InGaN quantum wells. These insights contribute to resolving the efficiency droop issue and offer valuable guidance for the design and optimization of next-generation high-efficiency light-emitting devices.

5. ACKNOWLEDGEMENT

The authors wish to express their gratitude to the Posts and Telecommunications Institute of Technology, Vietnam, for financial support for this research.

REFERENCES

Acuna, P. C., S. Leyre, J. Audenaert, Y. Meuret, G. Deconinck, and P. Hanselaer (2015). Impact of the Geometrical and Optical Parameters on the Performance of a Cylindrical Remote Phosphor LED. *IEEE Photonics Journal*, **7**(5); 1–14

Alaruri, S., A. Brewington, M. Thomas, and J. Miller (1993). High-Temperature Remote Thermometry Using Laser-Induced Fluorescence Decay Lifetime Measurements of Y_2O_3:Eu and YAG:Tb Thermographic Phosphors. *IEEE Transactions on Instrumentation and Measurement*, **42**(3); 735–739

Asano, T., T. Kondo, J. Yao, and W. Liu (2012). White Uniformity Evaluation of Electronic Displays Based on S-CIELAB Color System. In *2012 9th France-Japan & 7th Europe-Asia Congress on Mechatronics (MECATRONICS) / 13th International Workshop on Research and Education in Mechatronics (REM)*. pages 205–210

Chen, J., Z. Tian, Q. Wang, J. Liu, and Y. Mou (2021). Enhanced Color Rendering and Color Uniformity of PIG Based WLEDs by Using Red Phosphor Lens. *IEEE Photonics Technology Letters*, **33**(10); 471–474

Dong, X., F. Zheng, and Z. Wang (2021). Research on Color Uniformity and Seam Detection of Standard Test Paper Based on Machine Vision. In *2021 IEEE 4th Advanced Information Management, Communicates, Electronic and Automation Control Conference (IMCEC)*, volume 36. pages 1391–1395

Juntunen, E., O. Tapaninen, A. Sitomaniemi, and V. Heikkinen (2013). Effect of Phosphor Encapsulant on the Thermal Resistance of a High-Power COB LED Module. *IEEE Transactions on Components, Packaging and Manufacturing Technology*, **3**(7); 1148–1154

Kumar, H., S. Gupta, and K. S. Venkatesh (2018). Resolving Focal Plane Ambiguity Using Chromatic Aberration and Color Uniformity Principle. In *2018 IEEE 23rd International Conference on Digital Signal Processing (DSP)*. pages 1–5

Li, C. and Y. Li (2011). Color-Decoupled Photo Response Non-Uniformity for Digital Image Forensics. *IEEE Transactions on Circuits and Systems for Video Technology*, **22**(2); 260–271

Li, J., Y. Tang, Z. Li, J. Chen, X. Ding, and B. Yu (2018). Precise Optical Modeling of Phosphor-Converted LEDs with Arbitrary Concentration and Thickness Using Bidirectional Scattering Distribution Function. *IEEE Photonics Journal*, **10**(5); 1–17

Liang, S., Y. Jia, Z. Qin, and H. Sun (2011). Influences of Nutrient Concentration of Overlying Water on Nitrogen and Phosphor Release from Sediment in Lake Baiyangdian. In *2011 International Conference on Remote Sensing, Environment and Transportation Engineering*. pages 2225–2228

Liu, L., X. Tan, D. Teng, M. Wu, and G. Wang (2015). Simultaneously Enhancing the Angular-Color Uniformity, Luminous Efficiency, and Reliability of White Light-Emitting Diodes by *ZnO@SiO$_2$* Modified Silicones. *IEEE Transactions on Components, Packaging and Manufacturing Technology*, **5**(5); 599–605

Lu, X., W. Wang, Z. Su, S. Liu, and H. Zheng (2019). Phosphor Particle Spatial Patterning for High Angular Color Uniformity LED Packaging Through Selective Curing and Settling. In *2019 20th International Conference on Electronic Packaging Technology (ICEPT)*. pages 1–4

Miyazaki, H. and K. Kamei (1988). Measurement and Analysis of Color CRT Screen Uniformity. In *Conference Record of the International Display Research Conference*. pages 129–132

Reddy, P. S., R. A. R. Kumar, M. G. Mathews, and G. Amarendra (2017). Remote Online Performance Evaluation of Photomultiplier Tube and Electronics of DPCAM. *IEEE Transactions on Nuclear Science*, **64**(11); 2843–2853

Shalamanov, V., K. Simeonov, and N. Yaneva (2019). Examination of the Dynamic Variation of the Color Homogeneity of the Emitted Light From a Linear LED Luminaire With a Dynamic Color Adjustment of the Light. In *2019 Second Balkan Junior Conference on Lighting (Balkan Light Junior)*. pages 1–4

Shang, B., B. Xie, X. Yu, Q. Chen, and X. Luo (2015). An Improved Substrate Structure for High Angular Color Uniformity of White Light-Emitting Diodes. In *2015 16th International Conference on Electronic Packaging Technology (ICEPT)*. pages 1094–1097

Shin, M., R. Moon, J. Y. Lee, and Y. Kim (2013). Proposal and Design of Hybrid Light Guide Plate for Large-Area LED Display to Improve Illuminance and Color Uniformity. In *Microoptics Conference*. pages 1–2

Sun, C., Y. Chang, C. Lu, H. Lin, Z. Ting, T. Yang, and Y. Yu (2017). Spatial-Coded Phosphor Coating for High-Efficiency White LEDs. *IEEE Photonics Journal*, **9**(3); 1–9

Tain, Z., J. C. C. Lo, S. W. R. Lee, F. Yun, and R. Sun (2015). Investigation of the Influence of Ag Reflective Layer on the Correlated Color Temperature and the Angular Color Uniformity of LED With Conformal Phosphor Coating. In *2015 16th International Conference on Electronic Packaging Technology (ICEPT)*. pages 830–834

Takamura, S. and N. Kobayashi (2002). Practical Extension to CIELUV Color Space to Improve Uniformity. In *Proceedings of the International Conference on Image Processing*, volume 2. pages II–393–II–396

Wang, C., N. T. T. Khanh, and N. D. Q. Anh (2015). Improving the Correlated Color Temperature Uniformity of Multi-Chip White LEDs by *SiO$_2$* Scatters. In *2015 International Symposium on Next-Generation Electronics (ISNE)*. pages 1–4

Zhao, F., G. Dong, G. Yang, Y. Zeng, B. Shieh, and S. W. R. Lee (2020). Study on Light Emitting Surface Temperature of LEDs. In *2020 21st International Conference on Electronic Packaging Technology (ICEPT)*. pages 1–5

Zou, J., F. Han, Z. Zhang, H. Zheng, S. Liu, and S. Liu (2018). Fabrication of Phosphor Pillar Based on Electrohydrodynamic for High Angular Color Uniformity of White Light-Emitting Diodes. In *2018 19th International Conference on Electronic Packaging Technology (ICEPT)*. pages 1421–1425

